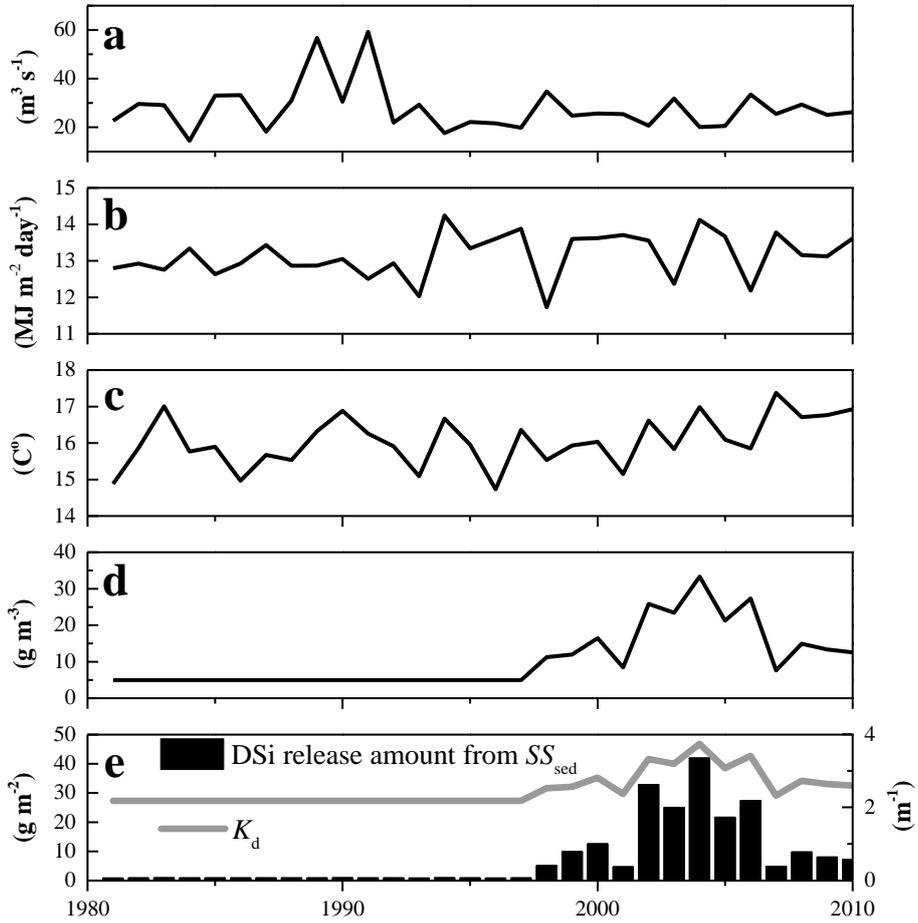# Supplementary figures

Fig. S1. Annual averages of model input variables such as discharge of the rivers inflowing the entire lake (**a**), daily solar irradiance (**b**), water temperature in BOX 3 (**c**), SS concentration derived from sediment resuspensin SS_{sed} in BOX 3 (**d**) and annual total amount of DSi released from SS_{sed} and annual mean light attenuation coefficient in water K_d estimated from SS_{sed} in BOX 3 (**e**).
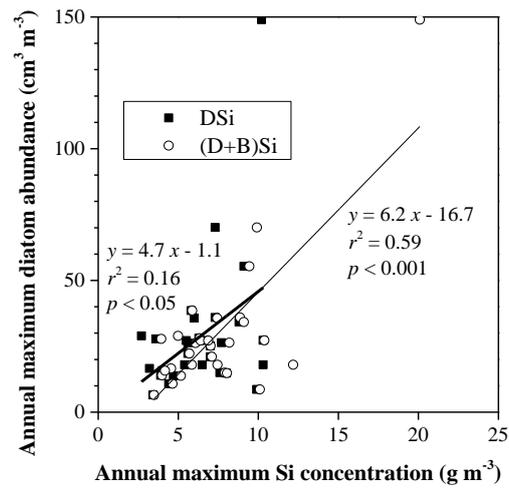
Fig. S2. Comparisons of the annual maximum DSi or (*D+B*) Si concentration with the

annual maximum diatom abundance observed at site C in Lake Kasumigaura.
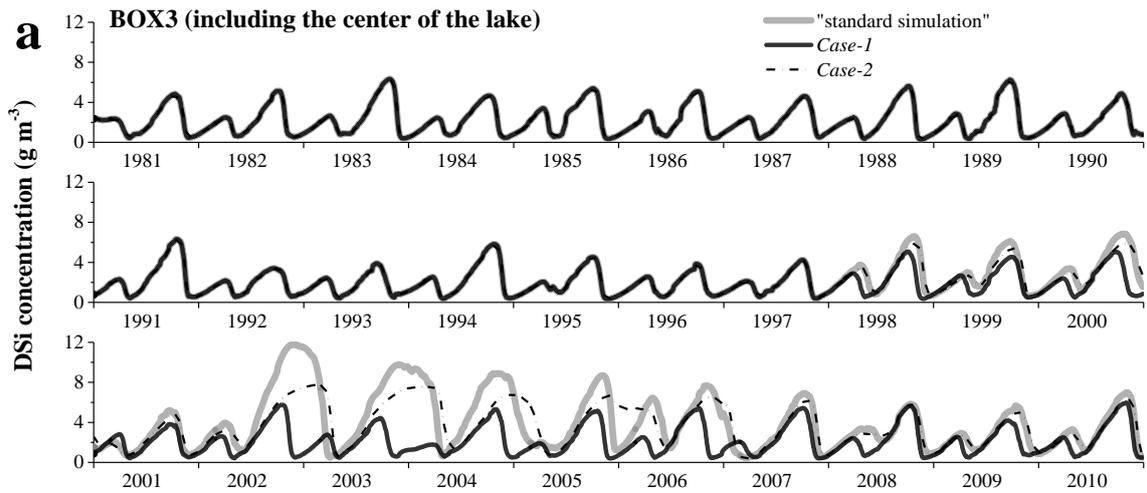
1
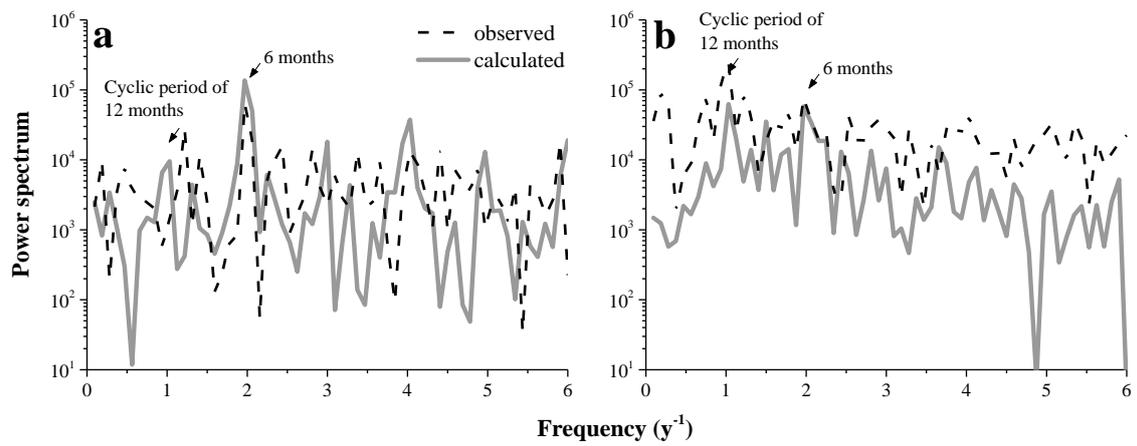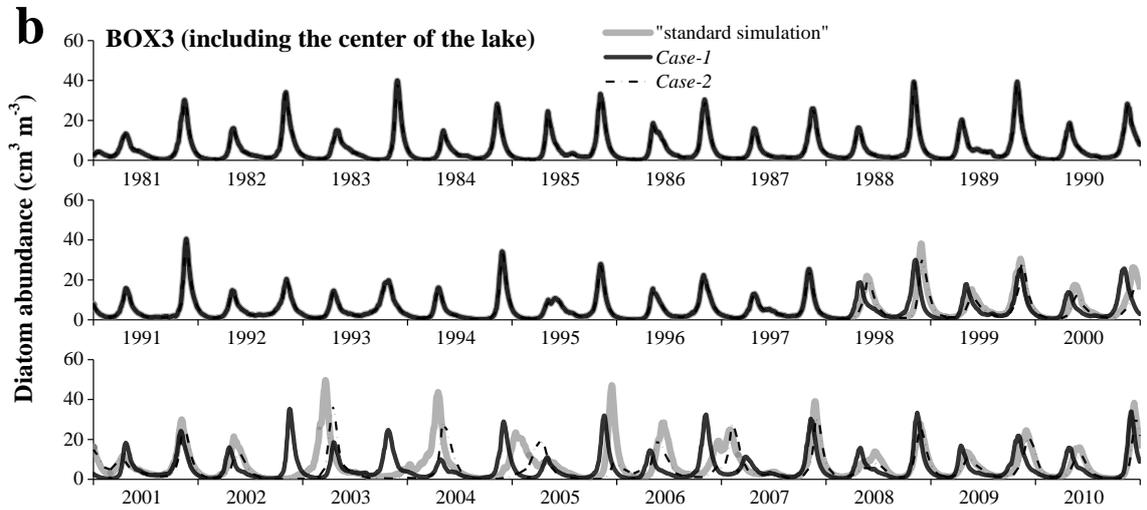
Fig. S3. Power spectrums of diatom abundance observed at site C and calculated by the model in BOX 3 during 1981–1990 (**a**) and 2001–2010 (**b**). Model predictions on the observation date were used for Fourier analysis.

a BOX3 (including the center of the lake)

"standard simulation"
Case-1
Case-2

DSi concentration (g m⁻³)

1981 1982 1983 1984 1985 1986 1987 1988 1989 1990

1991 1992 1993 1994 1995 1996 1997 1998 1999 2000

2001 2002 2003 2004 2005 2006 2007 2008 2009 2010

b BOX3 (including the center of the lake)

"standard simulation"
Case-1
Case-2

Diatom abundance (cm³ m⁻³)

1981 1982 1983 1984 1985 1986 1987 1988 1989 1990

1991 1992 1993 1994 1995 1996 1997 1998 1999 2000

2001 2002 2003 2004 2005 2006 2007 2008 2009 2010
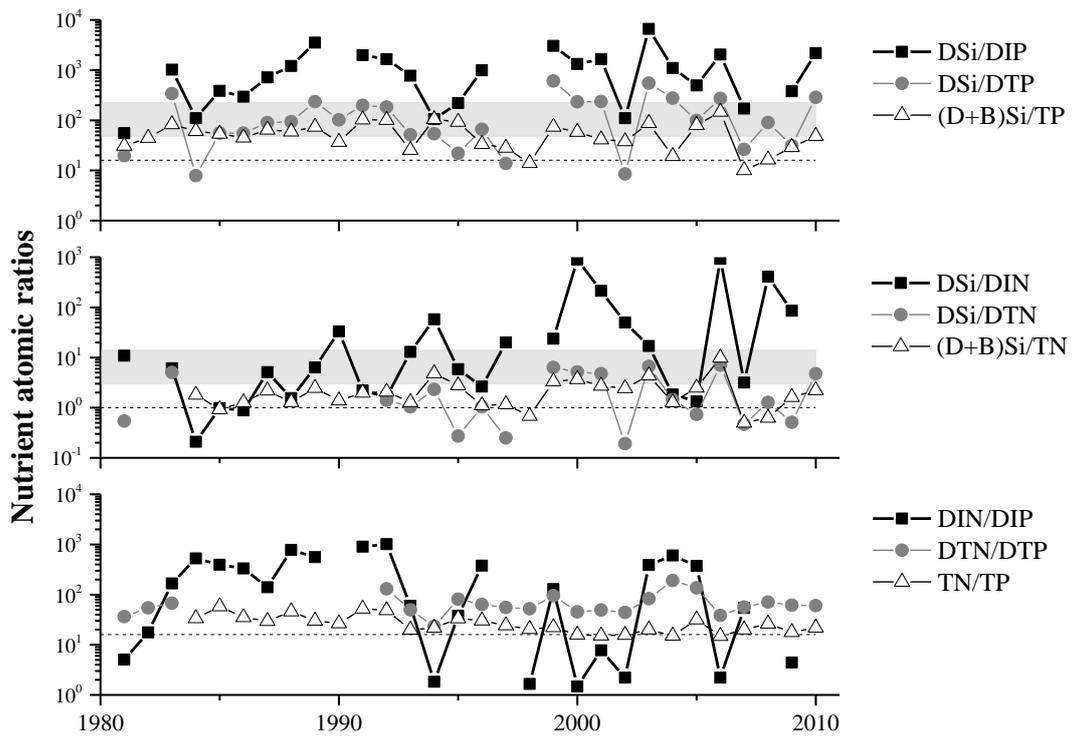
Fig. S4. Model predictions for DSi and diatoms in BOX 3 calculated by the standard simulation and by the simulation of Case 1 and 2.

Fig. S5. Long-term changes in the nutrient atomic ratios when annual maximum diatom abundance was observed at site C during 1981–2010. The gray zone and broken line indicates the nutrient atomic ratios of freshwater diatoms reported by Nagai *et al.* (2001) and of marine diatoms (Redfield ratio), respectively.